Journal of Energy in Southern Africa 26(3): 110–122
DOI: http://dx.doi.org/10.17159/2413-3051/2015/v26i2a2205

Thermodynamic analysis of a direct expansion solar assisted heat pump water heater

Masoud Yousefi

Misagh Moradali
Mechanical Engineering Department, South Tehran Branch, Islamic Azad University, Tehran, Iran

Abstract
In this paper, the thermodynamic performance of a direct expansion solar assisted heat pump (DX-SAHP), which is used to heat domestic water from 20 °C to 45 °C, is theoretically investigated. The system includes a 3m^2 single-cover flat plate solar collector, 0.150m^3 water tank and 70m tube immersed in the water tank as a condenser. The effect of various parameters such as radiation on the collector surface, compressor speed and the ambient temperature on the coefficient of performance (COP) are calculated. Results show that obtained COP is considerably more than that of a conventional heat pump water heater when radiation on the collector is high. Also, increasing collector area and reducing compressor speed enhance COP. The same occurs when the ambient temperature increases. For instance, at an ambient temperature of 15 °C and 450 w/m^2 irradiation on collector surface, the calculated COP was 6.37.

Keywords: solar, solar boosted, heat pump, water heater

Nomenclature

A_c	Collector area (m^2)
A_{coil}	Coil area (m^2)
cp_w	Water specific heat ($\frac{J}{kg\ k}$)
F	Collector efficiency factor
g	Acceleration due to gravity ($\frac{m}{s^2}$)
H	Coil convective heat transfer coefficient ($\frac{w}{m^2\ k}$)
h	Enthalpy ($\frac{J}{Kg}$)
K_w	Water conductive heat transfer ($\frac{w}{m^2\ k}$)
I	Solar irradiance ($\frac{w}{m^2}$)
L	Condenser length (m)
$\dot{m}$	Refrigerant mass flow rate ($\frac{kg}{s}$)
m_w	Water mass (Kg)
N	Compressor speed (RPM)
Q_e	Heat flow rate (w)
$Ra = g\,\beta\,\Delta T\ {L^3}/{\nu\lambda}$	Rayleigh number
VD	Compressor displacement volume (m^3)
Ta	Ambient temperature (°c)
Tp	Plate temperature (°c)
Tr	Refrigerant temperature (°c)
Tw	Water temperature (°c)
U_{LC}	Collector heat loss coefficient ($\frac{w}{m^2\ k}$)
Vw	Wind velocity ($\frac{m}{s}$)
W	Compressor power consumption (w)

Greek symbols

α	Absorptivity
β	Thermal expansion coefficient ($\frac{1}{k}$)
σ	Steffan-Boltzman constant
θ	Collector slope
εc	Glass emittance factor
εp	Plate emittance factor
ηv	Compressor volumetric efficiency
ν	Dynamic viscosity ($\frac{m^2}{s}$)
λ	Thermal diffusivity ($\frac{m^2}{s}$)
v	Refrigerant specific volume ($\frac{m^3}{kg}$)

1. Introduction

Due to growing energy demand and depletion of fossil fuel resources, the application of renewable energy resources has attracted a lot of interest. Among different renewable energy sources, solar energy is one of the best alternatives which is readily available in many parts of the world. Consequently, research and developments have been conducted to expand application of solar energy. Solar assisted heat pump is one these applications. The idea of combining conventional heat pumps and solar systems has taken many interests. As is well known, the COP of heat pumps improves by increasing the evaporator temperature. On the other hand, solar collectors work better if the plate

(absorber) temperature decreases. As a result, both systems operate better in comparison with working separately.

Grozable *et al.,* (2005) investigated the effect of using different refrigerants on the COP of a DX-SAHP. Using R22 and R134a instead of R12 decreased COP 2 to 4%. Replacement of R410a, R407C and R404a with R12 reduced COP 15 to 20%.

Kuang *et al.,* (2006) reported the results of analysis of a multi-functional DX-SAHP which offered space heating during winter and water heating the whole year. The system employed a 10.5 m^2 solar collector and variable speed compressor and could supply 0.200 to 1 m^3 hot water a day at 50 °C. The daily average heat pump COP was calculated between 2.6 to 3.3 for space heating only mode, while it varied from 2.1 to 2.7 for water heating only mode.

Guoying *et al.,* (2006) simulated the operating performance of a DX-SAHP for water heating. The system used a specially designed solar collector with spiral-finned tubes, which contributed to heat transfer from the air to the tubes. The effect of different parameters was analysed and the authors recommended using a variable speed compressor due to the wide range of operating conditions, namely, variable solar radiation.

Dickci et al., (2008) investigated experimentally a DX-SAHP which is used to heat a 60 m^2 residential building. The average COP of the system was 3.08 and the overall exergy loss was obtained to be 3.845 kW.

Chatuverdi et al., (2009) proposed to use two stage compressors for producing high temperature hot water in the range of 60-90 °C. Calculated COP was higher than that of a single-stage DX-SAHP.

Liu Keling *et al.,* (2009) presented a mathematical model and reported the results for the performance of a DX-SAHP where the compressor's power was supplied by photovoltaic panels. The system worked in the weather conditions of Tibet and had a variable frequency compressor. They found that in a sunny summer day, COP of the system reached to 6.01 and the average electric efficiency, thermal efficiency and overall efficiency were 0.135, 0.47 and 0.625, respectively.

Chow *et al.,* (2010) examined a DX-SAHP and simulated the long term performance of a model with typical meteorological data (TMY) for Hong Kong. The average yearly COP of the system was reported as 6.46. Results showed this system works better in summer where the COP reaches 10.

Dott, *et al*., (2012) simulated different combinations of solar heat pumps. An analytical study has been done on a solar assisted heat pump with carbon dioxide as the refrigerant (Raisul Islam and Sumathy, 2013). Recent research based on a life cycle cost analysis showed that DX-SAHP systems are economical as well as energy conserving compared to the conventional electrical water heaters (Chaturvedi, *et al*., 2014).

It is the aim of this paper to investigate the effect of operating parameters on the performance of a DX-SAHP used for water heating. Following an introduction of the system analysed, mathematical description of the system governing equations is presented and the effect of different contributing parameters in a sample system was analysed.

2. System description

Among different combinations, direct expansion solar assisted heat pumps (DX-SAHP) and indirect expansion solar assisted heat pumps (IX-SAHP) are the two more applicable systems. In an IX-SAHP, a fluid like water is heated in the solar system and then, in a heat exchanger, the process of heat transfer takes place between the heat pump evaporator and hot fluid to raise evaporator temperature. Figure 1 presents a schematic of IX-SAHP.

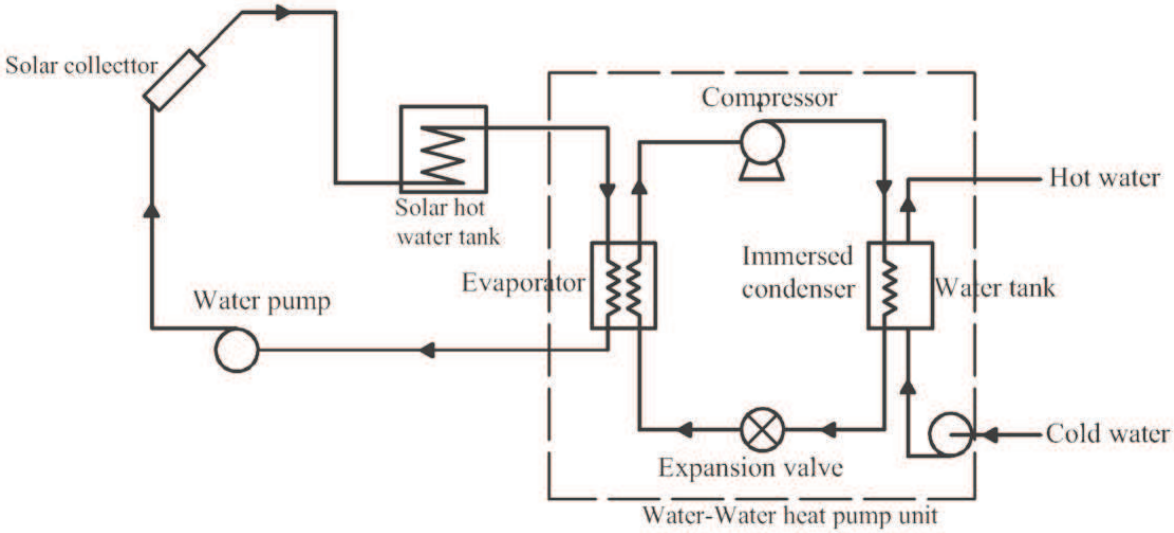

Figure 1: A schematic diagram of IX- SAHP

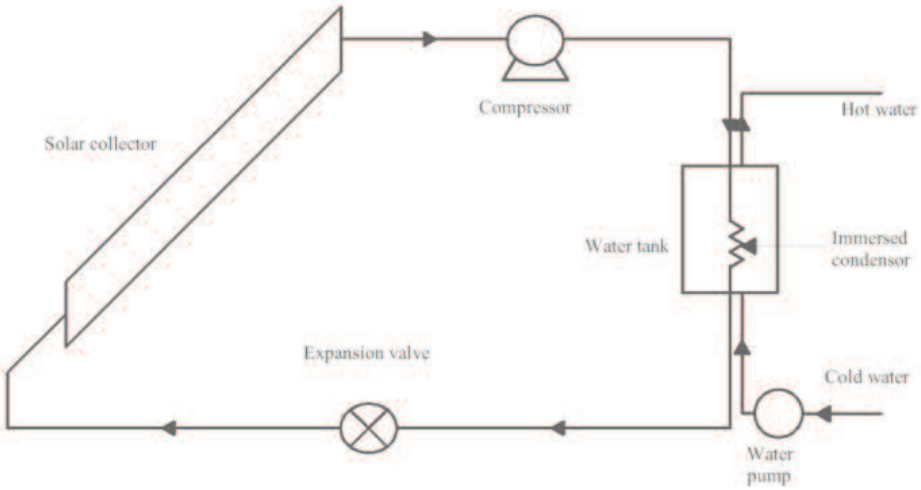

Figure 2: A schematic diagram of DX- SAHP

In a direct expansion solar assisted heat pump (DX-SAHP), solar collector tubes contain a refrigerant so it serves as the evaporator of system. Evaporation of refrigerant takes place by solar radiation and causes a decrease in plate temperature. Reduction of required components and risk of corrosion in the collector are two main advantages of this coupling. Figure 2 presents a schematic diagram of a DX-SAHP.

3. Mathematical model

A mathematical model is developed to predict the performance of a DX-SAHP. Except the water tank, quasi-steady modelling is used to model all components.

3.1 Solar collector

The solar energy collected by the collector/evaporator per unit area, Q_c, and the radiation heat transfer coefficient for one-cover solar collector, U_{LC}, are calculated as shown below (Duffie and Beckman, 2006):

$$Q_e = A_c(\alpha I - U_{LC}(t_p - t_a)) \quad (1)$$

$$Q_e = A_c F'(\alpha I - U_{LC}(t_r - t_a)) \quad (2)$$

$$U_{LC} = \left[\frac{1}{\frac{c}{t_P}\times\left(\frac{t_P - t_a}{1+f}\right)} + \frac{1}{h_w}\right]^{-1} + \left(\frac{\sigma(t_p + t_a)(t_p^{\,2} + t_a^{\,2})}{\frac{1}{\varepsilon_p + 0.0059\, h_w}} - 1\right) + \frac{1+f+0.133\,\varepsilon_p}{\varepsilon_c} \quad (3)$$

where:

$$f = (1 + 0.089\, h_w - 0.1166\, h_w\, \varepsilon_p)\times(1.07866) \quad (3\text{-a})$$

$$c = 520 \times (1 - 0.000051 \times \theta^2) \quad (3\text{-b})$$

$$e = 0.43 \times \left(1 - \frac{100}{t_p + 273}\right) \quad (3\text{-c})$$

Plate emittance factor (εp) and glass emittance factor (εc) are assumed to be 0.95 and 0.88, respectively. h_w is the convective heat loss coefficient and is equal to:

$$h_w = 2.8 + 3\, V_w \quad (4)$$

The energy balance equation in the collector/evaporator yields:

$$Q_e = \dot{m}(h_2 - h_1) \quad (5)$$

3.2 Compressor

The refrigerant mass flow rate is calculated by the following equation:

$$\dot{m} = \frac{\eta_v\, VD\, N}{60\, v} \quad (6)$$

The compressor power consumption is found by the energy balance equation:

$$w = \dot{m}(h_3 - h_2) \quad (7)$$

3.3 Condenser

The energy balance equation in condenser is expressed as:

$$Q_c = \dot{m}(h_4 - h_3) \quad (8)$$

The heat transfer coefficient of an immersed condenser can be calculated as shown below (Ji et al., 2010):

$$H = 0.685 \ (Ra)^{0.295} \frac{k_w}{L} \quad (9)$$

The heating capacity of the condenser is found by coil heat transfer coefficient:

$$Q_c = H A_{coil} (T_c - T_w) \quad (10)$$

Water tank temperature variation can be found from:

$$Q_c = m_w \, cp_w \frac{dt_w}{dt} \quad (11)$$

3.4 Expansion valve

The expansion valve process is assumed to be isentropic. So:

$$h_1 = h_4 \quad (12)$$

The heat pump coefficient of performance is obtained from:

$$COP = \frac{Q_h}{w} = \frac{h_4 - h_3}{h_3 - h_2} \quad (13)$$

All above equations are solved by MATLAB based on a flowchart shown in Figure 3. All thermodynamic properties are found by equations presented for R134a (Ji et al., 2010).

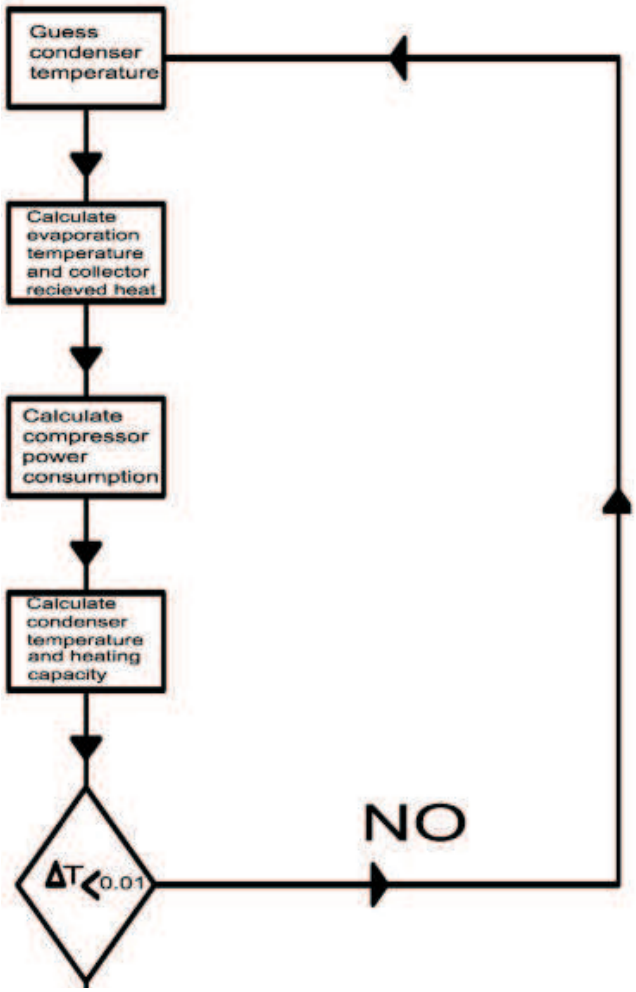

Figure 3: Calculation flow chart

4. System configuration

The above equations were solved for a system which is similar to some other previous experimental setups. Details of this system are described in Table 1.

Table 1: System configuration

Collector	One-cover flat plate collector F' =0.9, εC = 0.88, ερ = 0.95, θ = 35.5
Compressor	Reciprocating, VD= 24.1 cm^3 , ηv = 0.9, N= 1400 (rev/min)
Condenser	70m copper tube, Inner tube diameter = 8 mm, Outer tube diameter=12.5 mm

5. Results and discussions

Figure 4 shows the effect of solar irradiance and the average tank temperature on the performance of the system at 15°C ambient temperature and a wind velocity of 3 m/s. COP of the system increases when the received irradiance increases. In addition, reduction of water tank temperature results in increasing COP. The measured COP, when received radiation on the titled surface was 450 w/m^2, were calculated as 6.37, 5.16 and 4.28 at an average tank temperature of 20°C, 32.5°C and 45°C, respectively. At average water tank temperatures of 20°C, 32.5°C and 45°C and 950 w/m^2 radiation, the calculated COP were found to be 8.39°C, 6.62°C and 5.41°C, respectively.

Figure 5 shows system performance variation with ambient temperature. COP of the system boosts when the ambient temperature increases. The effect increases with increasing received irradiance.

At an ambient temperature of 10°C, and radiation values of 500, 700 and 900 w/m^2, COP was calculated as 6.52, 7.35 and 8.02, while at 20°C ambient and same received solar irradiance, calculated COP was 6.69, 7.55 and 8.25, respectively.

The variation of heat pump compressor power consumption with the received solar irradiance is presented in Figure 6. At 15°C ambient temperature and 450 w/m^2 solar irradiance, DX-SAHP power consumption was approximately 223.3, 347 and 347 W and at 950 w/m^2. These would change to 295, 378 and 468 W if the water tank temperature is taken as 20, 32.5 and 45, respectively.

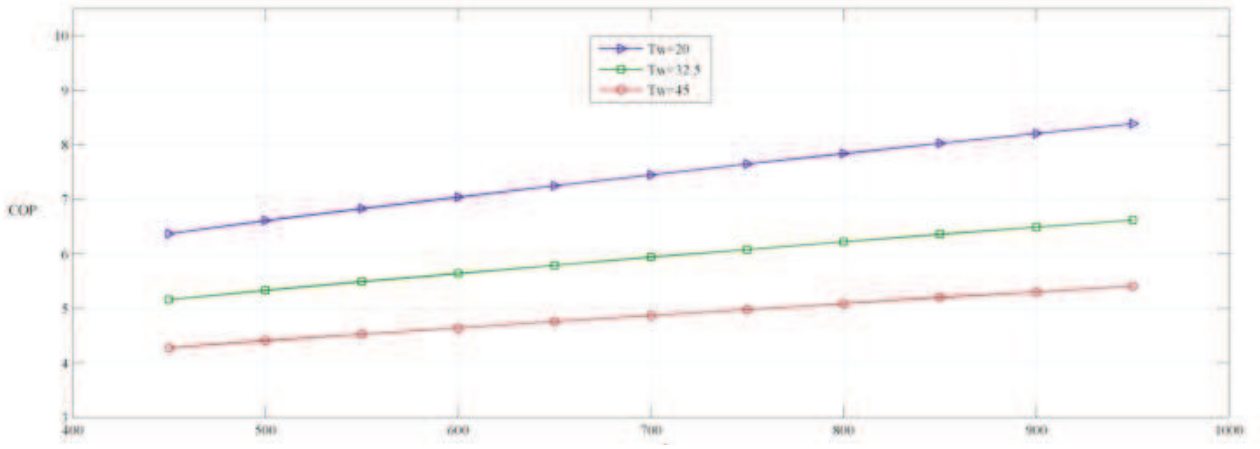

Figure 4: Variation of COP with solar irradiance

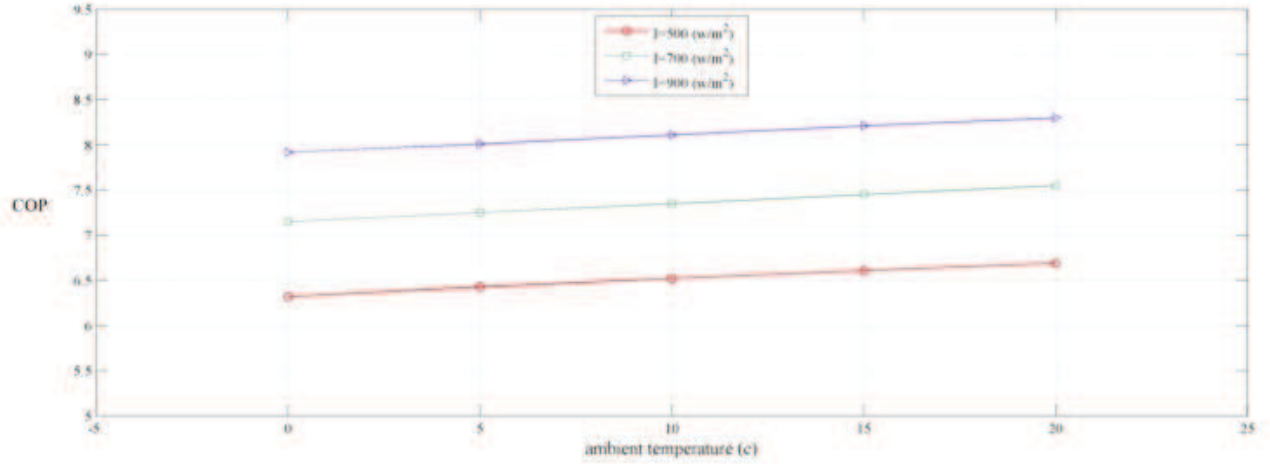

Figure 5: The effect of ambient temperature on COP

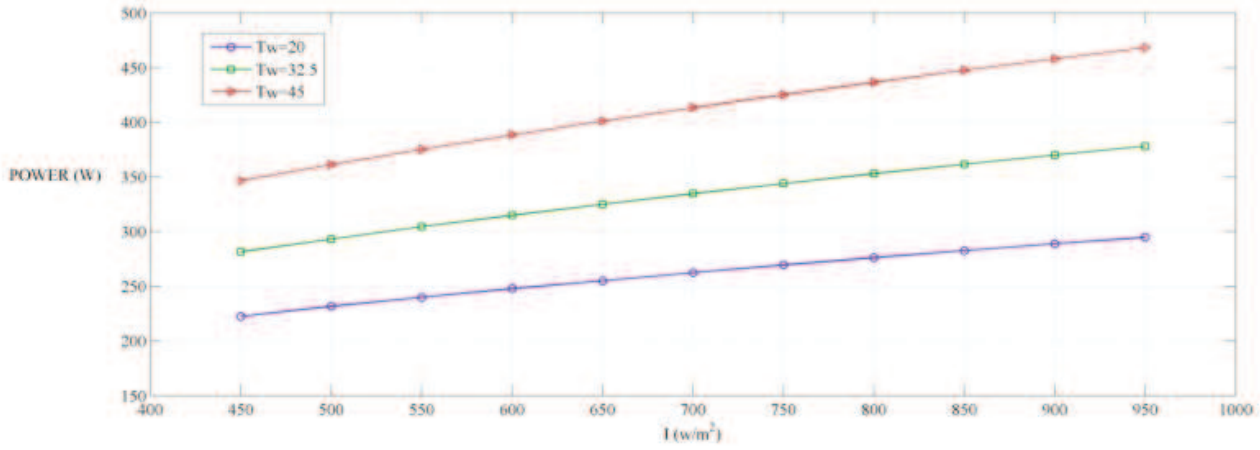

Figure 6: SAHP compressor power consumption

Figure 7 presents the effect of variation of compressor speed on the system at 15°C ambient temperature. Increasing compressor speed from 1100 rev/min to 1700 rev/min results in a reduction of coefficient of performance from 11 to 7 at 950 w/m^2 and from 7.64 to 6.72 at 450 w/m^2 when water tank temperature is 20 °C.

Figure 8 shows the improvement in the DX-SAHP coefficient of performance with increasing collector area. At 15°C ambient temperature and 20°C water tank temperature with 450 w/m^2 solar irradiance, calculated COP were 6.74 and 9.8 for collector area of 3.5 and 5 m^2, respectively.

Time required to heat 0.150 m^3 water is shown in Figures 9 to 11 in steady-state conditions when ambient temperature is assumed to be 15°C, compressor speed taken as 1400 rev/min with constant received solar irradiance. According to the calcula-

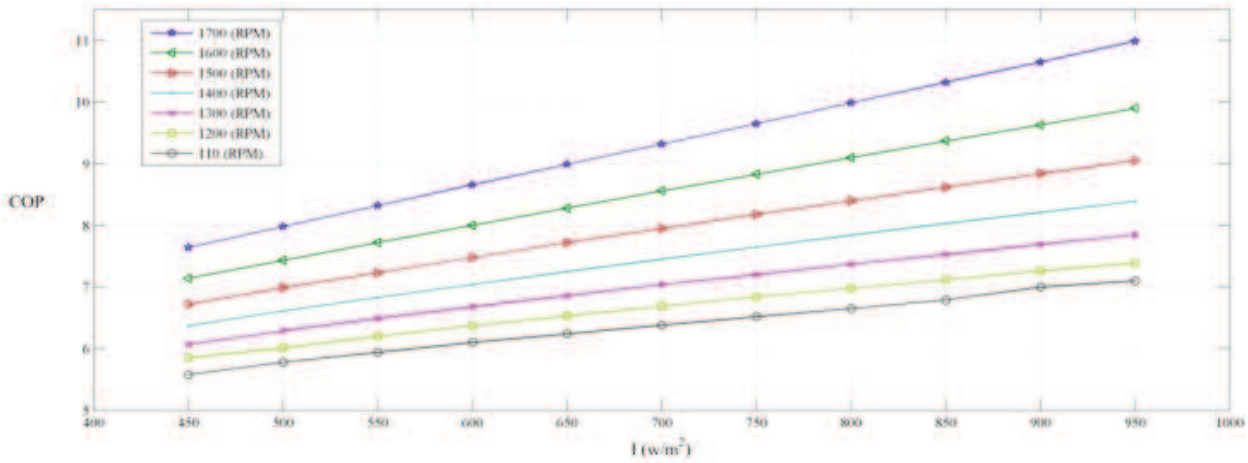

Figure 7: Effect of compressor speed on the performance of SAHP

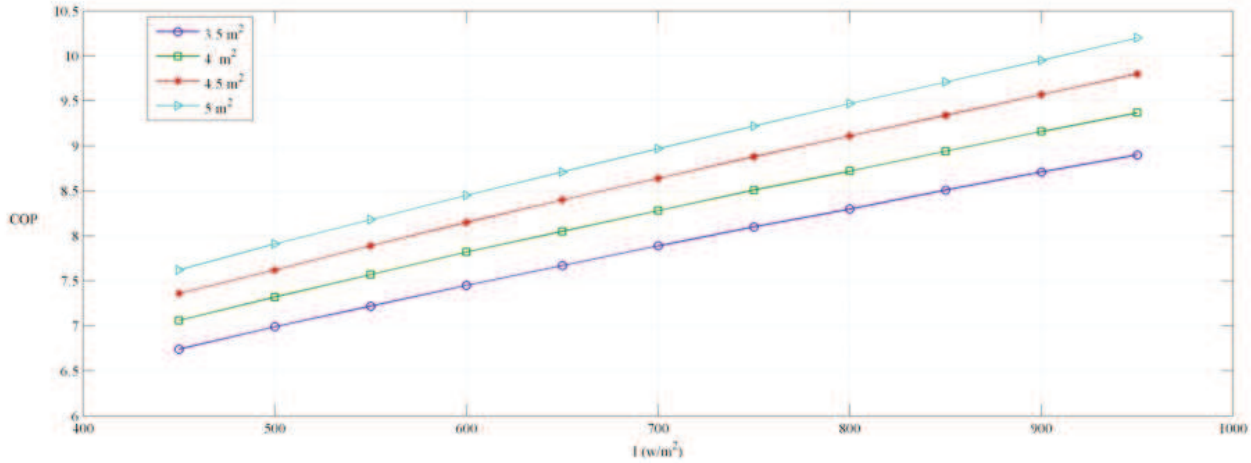

Figure 8: The effect of collector area on the performance

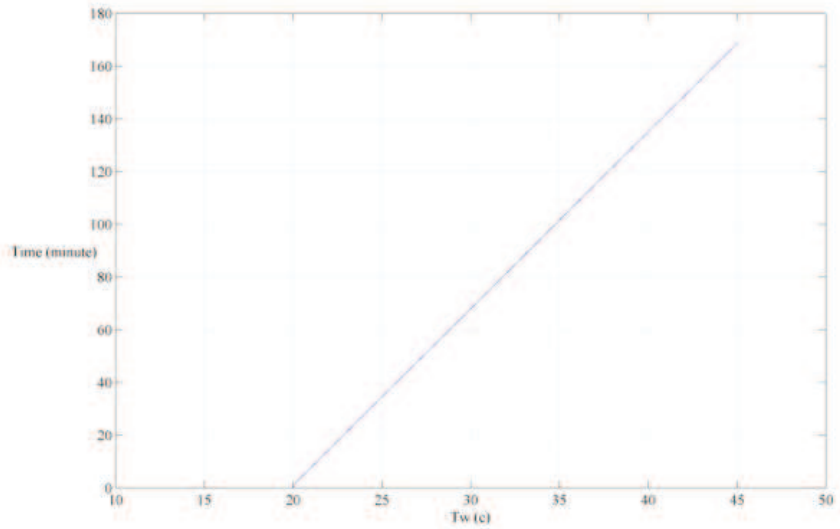

Figure 9: Variation of water tank temperature with time in 500 w/m^2

tion at 500, 700 and 900 w/m^2 irradiation, the heating process takes 169, 132 and 112 minutes, respectively.

6. Conclusion

The results of simulation and thermodynamic analysis of a solar assisted heat pump water heater with a 0.150 m^3 water tank was presented. Effective parameters on the performance of the system was investigated which included solar irradiance, ambient temperature, compressor speed and solar collector area. According to the results, increasing solar irradiance and ambient temperature, reducing water tank temperature and compressor speed, all

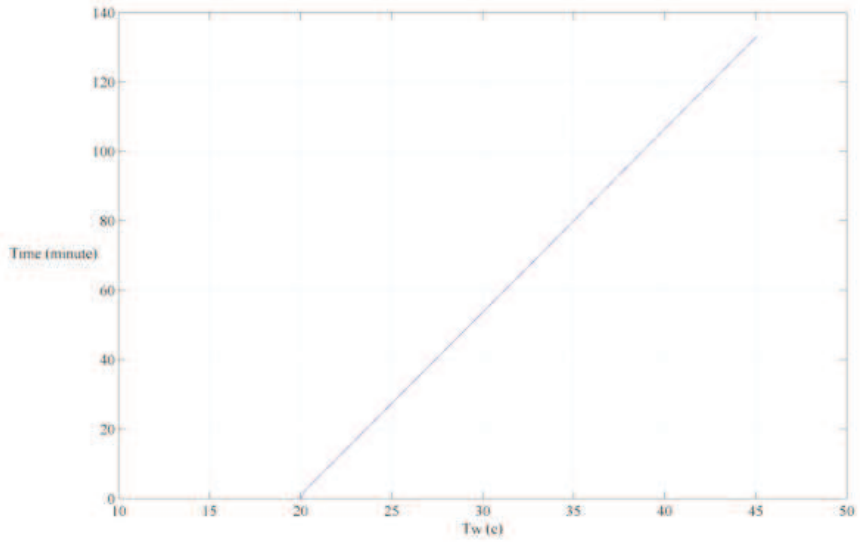

Figure 10: Variation of water tank temperature with time in 700 w/m^2

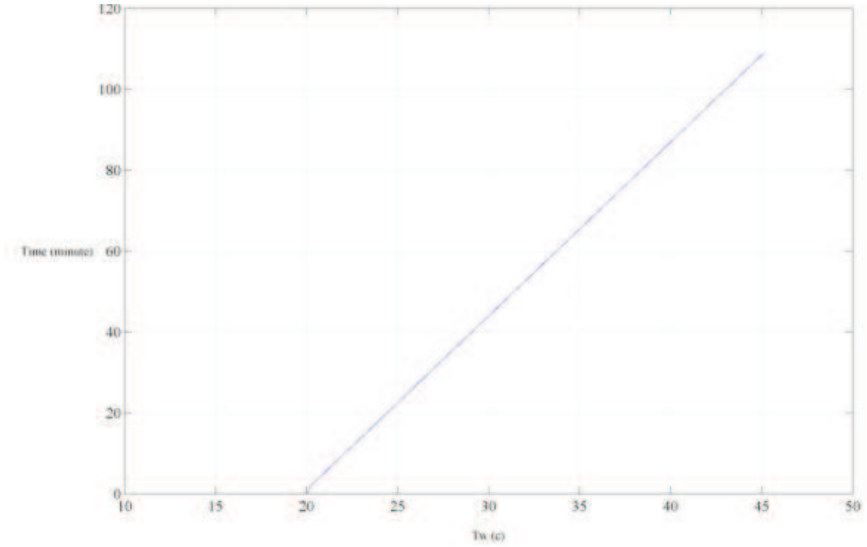

Figure 11: Variation of water tank temperature with time in 900 w/m^2

enhance the coefficient of performance. System COP was found to be 6.37 and 8.39 at solar irradiance values of 450 and 950 w/m^2, Table 1 Fuzzy controller rules for temperature controlrespectively. This is higher in comparison with that of a conventional heat pump water heater.

Acknowledgements

The authors would like to acknowledge the financial support of the Islamic Azad University, South Tehran Branch.

References

Chaturvedi, S.K., *et al.* (2009). Two-stage direct expansion solar-assisted heat pumps for high temperature application. *Applied Thermal Engineering*, 29: 2093-2099.

Chaturvedia, S.K., Gagranib, V.D. and Abdel-Salam, T.M. (2014). Solar-assisted heat pump – A sustainable system for low-temperature water heating applications. *Energy Conversion and Management*. 77: 550-557.

Chow, T.T., *et al.* (2010). Modelling and application of direct-expansion solar-assisted heat pump for water heating in subtropical Hong Kong. *Applied Energy*. 87: 643-649.

Cleland, A.C. (1994). Polynomial curve-fits for refrigerant thermodynamic properties: extension to include R134a. *International Journal of Refrigeration*. 17: 245-249.

Dikci, A., and Akbulut, A. (2008). Performance characteristics and energy-exergy analysis of solar assisted heat pump. *Building and Environment*. 43: 1961-1967.

Dott, R., Genkinger, A., and Afjei, T. (2012). System evaluation of combined solar and heat pump systems. *Energy Procedia*, 30: 562-570.

Duffie, J.A., and Beckman, W.A. (2006). Solar engineering of thermal processes. Third edition. John Wiley and Sons Inc.

Gorozabel, F.B., *et al.* (2005). Analysis of direct expan-

sion solar assisted heat pump using different refrigerant. *Energy Conversion and Management*. 46: 2614-2624

Guoying Xu, Xiaosong Zhang, Shiming Deng. (2006). A simulation study on the operating performance of a solar-air source heat pump water heater. *Applied Thermal Engineering*. 26: 1257-1265

Ji, J., *et al.* (2010). Performance analysis of an air source heat pump using an immersed condenser. *Frontiers of Energy and Power Engineering*. 4: 234-245.

Keling, L., *et al.* (2009). Performance study of a photovoltaic solar assisted heat pump with variable-frequency compressor- A case study in Tibet. *Renewable Energy*. 34: 2680-2687.

Kuang, Y.H., and Wang, R.Z. (2006). Performance of multi-functional direct-expansion solar assisted heat pump. *Solar Energy*. 80: 795-803.

Received 11 May 2014; revised 27 April 2015